Metal-insulator transition in Co-doped ZnO: Magnetotransport properties

Qingyu Xu,* Lars Hartmann, Heidemarie Schmidt, Holger Hochmuth, Michael Lorenz, Rüdiger Schmidt-Grund, Chris Sturm, Daniel Spemann, and Marius Grundmann

Institut für Experimentelle Physik II, Fakultät für Physik und Geowissenschaften, Universität Leipzig, Linnéstrasse 5, D-04103 Leipzig, Germany

(Received 6 February 2006; revised manuscript received 10 April 2006; published 23 May 2006)

The magnetotransport properties [magnetoresistance (MR) and Hall effect] of Co-doped ZnO films prepared by pulsed laser deposition have been investigated around the metal-insulator transition (MIT) as a function of temperature (from 5 to 290 K) under a maximum magnetic field strength of 6 T. From the MR behavior measured at 5 K we conclude that the MIT occurs at the critical electron concentration $n_c \approx 4\times10^{19}$ cm^{-3}. At 5 K we observed positive MR in the insulating regime ($n<n_c$) and negative MR in the metallic regime ($n>n_c$). Furthermore, in the transition regime of the MIT ($n\sim n_c$) negative MR at low magnetic field and positive MR at high field was observed. We consider the critical electron concentration n_c as an important material parameter because n_c does not depend on film thickness or Co content. The anomalous Hall effect being of importance for future spintronic materials was only clearly observed in Co-doped ZnO with $n<n_c$.

DOI: 10.1103/PhysRevB.73.205342 PACS number(s): 75.50.Pp, 75.47.De, 73.61.Ga, 71.30.+h

Diluted magnetic semiconductors (DMSs) have attracted much attention for their potential areas of applications in spintronics.[1] Following the theoretical prediction of room-temperature ferromagnetism in ZnO-based DMSs,[2] 3*d* transition-metal- (TM-)doped ZnO has been studied intensively to achieve room-temperature ferromagnetism. Besides ferromagnetic magnetization, the ZnO-based DMSs also exhibit interesting magnetotransport phenomena. Both positive and negative magnetoresistance (MR) were observed, depending on TM doping, film thickness, and measuring temperature.[3,4] The anomalous Hall effect (AHE) was also observed in Co- and Mn-doped ZnO films.[4,5] A spin coherence time as long as 1 ns has been found by measuring low-temperature MR on undoped and Mn-doped ZnO and a coupling constant amounting to $\lambda_{so}=(4.4\pm0.4)\times10^{-11}$ eV cm.[6] However, more work is still needed to understand the magnetotransport properties in ZnO-based DMSs at elevated device operating temperatures.

It is known that magnetotransport properties of magnetic semiconductors strongly depend on the charge carrier concentration,[7,8] which are electrons in intrinsically *n*-conducting ZnO. With decreasing electron concentration, at the metal-insulator transition (MIT), the character of wave functions changes from delocalized to localized. In this paper, we study the MR and Hall effect of Co-doped ZnO films in dependence on the free-electron concentration *n*. For a critical electron concentration n_c we probed the MIT and related changes of MR in Co-doped ZnO.

The Co-doped ZnO films were grown from a $Zn_{0.945}Co_{0.05}Al_{0.005}O$ pulsed laser deposition (PLD) target on 10×10 mm^2 *a*-plane sapphire substrates by pulsed laser deposition using a KrF excimer laser. The distance between PLD target and substrate amounted to 10 cm. The film thickness was controlled by the number of the laser pulses with an energy density of 2 J cm^{-2} and *ex situ* determined by modeling spectral ellipsometry data measured in the energy range of 1–4 eV.[9] Different temperatures at the substrate holder and film thickness were chosen to vary the electron concentration by several orders of magnitude around the critical electron concentration n_c. The PLD target was prepared by mixing and pressing appropriate amounts of ZnO (99.9%), CoO (99.999%), and Al_2O_3 (99.998%) powders. 0.5 mol % Al was included in the PLD target to fabricate conductive thin films. The resulting composition of the films was determined by combined Rutherford backscattering spectrometry and particle-induced x-ray emission measurements and is given together with substrate temperature in Table I. Due to the underlying substrate, the Al content in the Co-doped ZnO films could not be determined. When decreasing the substrate holder temperature from 820 to 390 °C, the Co content in the deposited films decreases gradually from ~10% to ~7%, nevertheless being larger than the nominal Co content in the target.

The crystal structure of the films was characterized by x-ray diffraction measurements with θ-2θ scans using a Cu $K\alpha$ source. Only (002) and (004) peaks of wurtzite ZnO were observed, indicating that the Co-doped ZnO films are

TABLE I. PLD substrate temperature and thickness of Co-doped ZnO film. All films have been grown at an oxygen partial pressure amounting to 4×10^{-5} mbar. The film prepared at a substrate temperature of 824 °C is an insulator. The nominal composition of the PLD target used was $Zn_{0.945}Co_{0.05}Al_{0.005}O$. The letters in parentheses (*n* column) indicate whether the sample is in the insulating (I), transition (T), or metallic (M) regime.

$T_{substrate}$ (°C)	Thickness (nm)	*n* at 5 K (cm^{-3})	Co-content (at. %)
824			10.1
729	689	1.7×10^{19} (T)	10.0
689	261	5.1×10^{18} (I)	9.8
638	269	4.0×10^{19} (T)	9.5
591	144	3.7×10^{19} (T)	9.1
530	64	9.8×10^{19} (M)	9.0
460	38	1.3×10^{20} (M)	6.7
390	26	9.9×10^{19} (M)	7.0

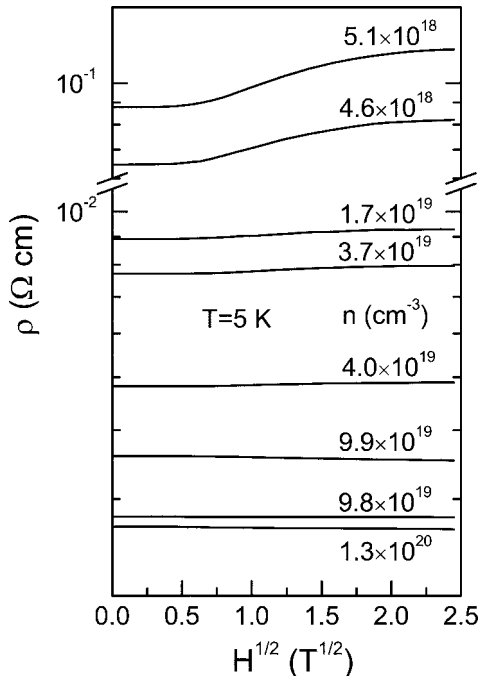

FIG. 1. Resistivity of Co-doped ZnO as a function of the square root of the magnetic field at 5 K for selected electron concentrations ranging from 4.6×10^{18} ($n<n_c$) to 1.3×10^{20} cm^{-3} ($n>n_c$).

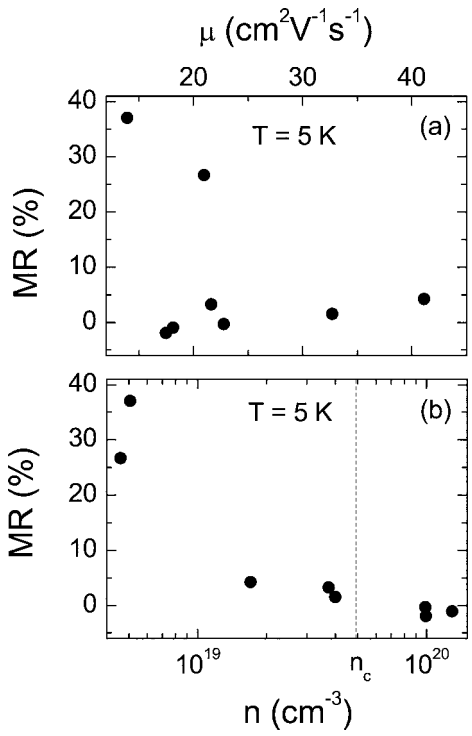

FIG. 2. The MR value at maximum field 6 T for the samples from Fig. 1 in dependence on (a) electron mobility μ and (b) concentration n at 5 K. The critical electron concentration $n_c=4.9\times10^{19}$ cm^{-3} determined using Eq. (1) is also indicated.

highly c-axis oriented, without any magnetic or nonmagnetic precipitates being larger than 10 nm. The magnetic field dependence of resistivity and Hall effect was measured with the field applied parallel to the c axis of the films (perpendicular to film surface) in the van der Pauw configuration. Fields up to 6 T were applied over a wide temperature range from 5 to 290 K. The type of the conducting carriers was confirmed to be n type by Hall measurements for all the samples.

Figure 1 shows the resistivity of Co-doped ZnO films as a function of the square root of the magnetic field measured at 5 K for a wide range of electron concentrations n. It is known that electronic properties of n-conducting semiconductors sensitively depend on the ratio of the mean distance between donors $r=(3/4\pi n)^{1/3}$ to their effective Bohr radius a_B. In the dilute case, $r\gg a_B$, electrons are bound to individual impurities, and low-temperature conduction proceeds by means of phonon-assisted tunneling between occupied and empty states. The semiconductor is said to be in the insulating regime. In the opposite limit, $r\ll a_B$, electrons reside in the conduction band, and low-temperature mobility is determined by ionized impurity scattering. The critical electron concentration n_c where the MIT happens can be estimated from $r=a_B$; thus,

$$n_c=\left(\frac{0.62}{a_B}\right)^3. \tag{1}$$

In a Co-doped ZnO film, Co isovalently substitutes for Zn, and MIT can be estimated from Eq. (1). With a_B amounting to 1.7 nm for ZnO, n_c can be calculated to be 4.9×10^{19} cm^{-3}. From the estimated n_c, we expect delocalized and localized wave functions for $n\geq4.9\times10^{19}$ and $n\leq4.9\times10^{19}$ cm^{-3}, respectively. It can be clearly seen that for electron concentration n smaller than 10^{19} cm^{-3}, strong positive MR can be observed, while for an electron concentration larger than 10^{19} cm^{-3}, small negative MR was observed.

In order to reveal a possible dependence of the MR behavior on electron concentration or mobility μ, the MR values at the maximum field 6 T from the MR curves in Fig. 1, namely, $[R(6\text{ T})-R(0\text{ T})]/R(0\text{ T})$, are plotted as a function of n and μ in Fig. 2. No clear relation between MR and electron mobility may be detected [Fig. 2(a)]. However, with decreasing electron concentration n [Fig. 2(b)], the MR changes sign, finally reaching a positive value of MR=37% for $n=5.1\times10^{18}$ cm^{-3}. The MR changes sign at $n\approx4\times10^{19}$ cm^{-3}, where the MIT is theoretically predicted using Eq. (1). The thinnest investigated film has a thickness of 26 nm. The mean free path of the electrons is estimated to be less than 2 nm, which is small compared to the film thickness.[10] Therefore we think that bulk properties are reached and n_c does not depend on the film thickness. In order to determine n_c more precisely, more Co-doped ZnO samples with n around n_c should be investigated. As can be seen from Fig. 3(b), negative MR at low field and positive MR at high field can be observed for $n\sim n_c$. The typical MR curves at 5 K for the selected samples in insulator, transition, and metallic regimes are shown in Fig. 3.

Kim *et al.*[3] observed the same positive MR below ($n=5.1\times10^{19}$ cm^{-3}) and negative MR above ($n=9.2\times10^{20}$ cm^{-3}) n_c in Co-doped ZnO with high and low Co doping. For $n\sim n_c$ ($n=7.5\times10^{19}$ cm^{-3}) they reported nega-

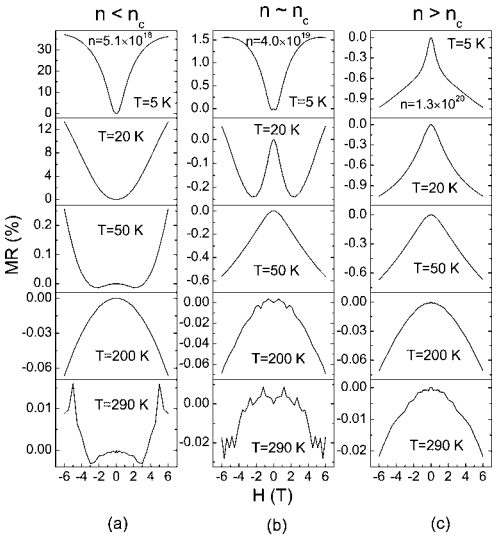

FIG. 3. The MR as a function of the magnetic field measured on Co-doped ZnO at 5 K with (a) $n<n_c$ ($n=5.1\times10^{18}$ cm^{-3}), (b) $n\sim n_c$ ($n=4.0\times10^{19}$ cm^{-3}), and (c) $n>n_c$ ($n=1.3\times10^{20}$ cm^{-3}).

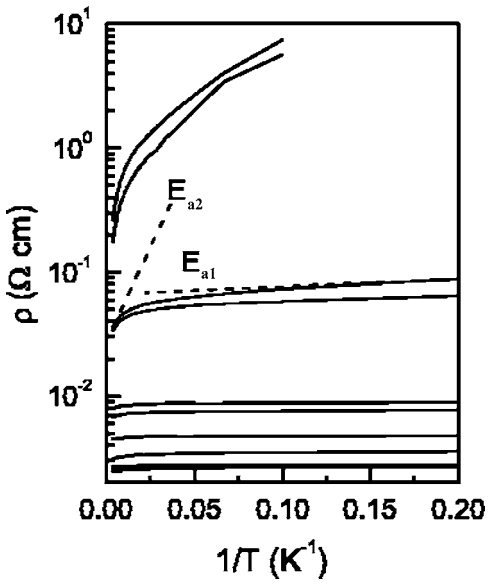

FIG. 4. Variation of ρ in logarithmic scale versus $1/T$ measured on Co-doped ZnO films in metallic, transition, and insulating regime. The dashed lines indicate the linear fitting for the thermal activation energy.

tive MR at low field and positive MR at higher field with intermediate Co doping.

Figures 3(a)–3(c) summarize the temperature dependence of MR for Co-doped ZnO films in the insulating, transition, and metallic regimes, respectively. For the insulating film, only positive MR was observed at 5 and 20 K. At 50 K, negative MR can be observed at low magnetic field. At 200 K only negative MR was observed. However, small positive MR can still be observed at 290 K. In the metallic regime, only negative MR can be observed. Here the MR decreases from 5 to 290 K. For the film in the transition regime of n_c at 5 and 20 K, negative MR was observed at low field and positive MR at high field. On further increasing the temperature, only negative MR was observed.

The resistivity of the films was measured from 5 to 290 K at zero magnetic field. In Fig. 4, the resistivity ρ is represented on a logarithmic scale as a function of reciprocal temperature, in order to represent the modeled thermal activation energy E_a for the activation of charge carriers into the conduction band. In the simplest case, we expect

$$\ln \rho = \frac{E_a}{k_B}\frac{1}{T} + \ln \rho_0, \tag{2}$$

where k_B is the Boltzmann constant and ρ_0 a temperature-independent contribution to the resistivity. In case of only Al donors, the modeled activation energy E_a should be 65 meV.[11] In Fig. 4 dashed lines show the curves of ρ versus $1/T$ to be modeled in the low-temperature range with activation energy E_{a1} and high temperature range with activation energy E_{a2}. In the metallic range with ρ smaller than 10^{-2} Ω cm, E_{a1} and E_{a2} are smaller than 1 meV. Therefore even at room temperature the Fermi level lies close to the conduction band. Both modeled activation energies increase with decreasing electron concentration. In the insulating range with ρ larger than 10^{-1} Ω cm, the modeled activation energy E_{a1} and E_{a2} amounts to 1.6 and 18 meV, respectively.

We would like to state that the free charge carriers in the metallic and transition regimes are mainly generated by the ionization of very shallow donors with $E_a<1$ meV. Note that a thermal activation energy in Mn-doped ZnO amounting to 1.5 meV was attributed to the activation energy from an impurity band to the conduction band.[5]

Finally, we probed the Hall voltage in the temperature range from 5 to 290 K. A well-known ferromagnetic response of charge carriers in ferromagnetic semiconductors is the AHE. The Hall resistivity ρ_{xy} is known to be a sum of ordinary and anomalous Hall terms, $\rho_{xy}=R_0B+R_s\mu_0M$ where B is the magnetic induction, μ_0 is the magnetic permeability, M is the magnetization, R_0 is the ordinary Hall coefficient, and R_s is the anomalous Hall coefficient. The first is the ordinary Hall effect, linear in B, and the second is the AHE proportional to M.[12] The anomalous Hall term is conventionally attributed to asymmetric scattering processes involving a spin-orbit interaction between the conduction electrons and the magnetic moments in the material. The field dependence of ρ_{xy} is shown in Fig. 5. The data were obtained by a simple subtraction $\rho_{xy}=\frac{1}{2}[\rho_{xy}(H)-\rho_{xy}(-H)]$ in order to eliminate any magnetic-field effects which are an even function of field, i.e., MR.

In the insulating regime, the AHE was clearly observed at low temperature. Figures 5(a) and 5(b) show the Hall curve for two samples, the sample A with n of 6.7×10^{17} cm^{-3} at 20 K [Fig. 5(a)] and the sample B with n of 5.1×10^{18} cm^{-3} at 5 K [Fig. 5(b)]. The ordinary Hall term can be determined by linear fitting of the high-field Hall data where the anomalous Hall term has saturated. By subtracting the ordinary Hall term, only the anomalous Hall term which mimics the magnetization curve is left and is shown in the insets of Fig. 5. It can be clearly seen that the anomalous Hall resistivity saturates at a value ρ_{xys}. It must be noted that the Hall resistivity was noisy for samples with $n\ll n_c$ due to

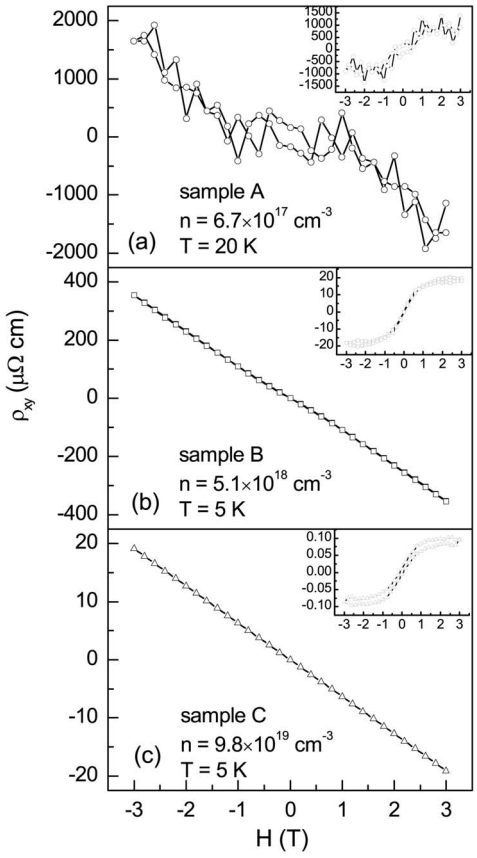

FIG. 5. Hall resistivity versus magnetic field for sample *A* with n of 6.7×10^{17} cm^{-3} at 20 K (a), sample *B* with n of 5.1×10^{18} cm^{-3} at 5 K (b), and sample *C* with $n=9.8\times10^{19}$ cm^{-3} at 5 K. The insets show the anomalous Hall resistivity in which the ordinary Hall contribution is subtracted.

the too large resistance and the large MR effect. ρ_{xys} for sample *A* amounts to 896 $\mu\Omega$ cm, which is much larger than that for sample *B*(20 $\mu\Omega$ cm). It can be clearly seen that with decreasing electron concentration, the AHE is strongly enhanced. For the sample with $n>n_c$, no clear AHE can be observed. Figure 5(c) shows the Hall curve for sample *C* with $n=9.8\times10^{19}$ cm^{-3}. However, by subtracting the ordinary Hall term as in Figs. 5(a) and 5(b), a small AHE still can be observed, shown in the inset of Fig. 5(c). But ρ_{xys} is only 0.09 $\mu\Omega$ cm, which is much smaller than that of samples *A* and *B* with $n<n_c$.

The doping of a 3*d* TM will induce a giant *s*-*d* exchange interaction in magnetic oxide semiconductors, leading to spin splitting of the *s*-type conduction band. In the metallic range, the spin splitting is smaller than the Fermi energy.[7] And the magnetic-field-induced redistribution of electrons between the spin-split subbands is small. Thus its effect on the resistivity is small. The negative MR in the metallic regime reflects that the spins of the doped magnetic ions will tend to be aligned parallel under the applied magnetic field and thus the magnetic scattering of the doped magnetic ions was suppressed. With decreasing electron concentration, the redistribution of electrons between the spin-split conduction-band minimum will significantly influence the conductivity due to spin-disorder scattering, orbital effects and formation of bound magnetic polarons which originate from the scattering-modified electron-electron interactions, leading to the positive MR.[7,13] Large spin splitting in the insulating regime was also manifested by the clear observation of the AHE, which is proportional to the spin polarization of the electron gas. Because the spin splitting is proportional to the macroscopic magnetization induced by the Co ions, the observed positive MR and AHE in the insulating regime suggest that the ferromagnetism may be realized in the Co-doped ZnO with low electron concentration. This conclusion is also supported by the recently observed giant magnetic moment of $6.1\mu_B$/Co and high Curie temperature of 790 K in ferromagnetic insulator (4 at. %) Co-doped ZnO. The bound magnetic polaron model gives one plausible explanation.[14] In order to prepare ferromagnetic Co-doped ZnO for use in future spintronic devices, the chemical origin of very shallow donors and its influence on the total free-electron concentration has to be systematically studied. Furthermore, also for Mn-doped ZnO it would be of interest to investigate the magnetotransport properties in the transition regime of the MIT, which is currently under study.

In summary, a critical electron concentration ($n_c=4\times10^{19}$ cm^{-3}) has been determined from the MR properties of Co-doped ZnO prepared by PLD on *a*-sapphire substrates. We observed positive MR in the insulating regime ($n<n_c$) and negative MR in the metallic regime ($n>n_c$). Furthermore, in the transition regime of the MIT ($n\sim n_c$) negative MR at low magnetic field and positive MR at high field was observed. With increasing temperature, n increases and subsequently the positive MR decreases abruptly and negative MR emerges at low magnetic field. The AHE may only be clearly observed in insulating Co-doped ZnO films. The observed positive MR and AHE suggest that ferromagnetic Co-doped ZnO may be realized if the electron concentration lies below 10^{19} cm^{-3}.

This work is financially supported by BMBF (Grant No. FKZ03N8708). The authors would like to thank J. Lenzner, R. Riedel, and M. Ziese for help with magnetotransport equipment, G. Ramm for the target preparation, and H. von Wenckstern and M. Brandt for help with the software.

*Corresponding author. Email address: xuqingyu_1974@yahoo.com

[1] H. Ohno, Science **281**, 951 (1998).

[2] T. Dietl, H. Ohno, F. Matsukura, J. Cibert, and D. Ferrand, Science **287**, 1019 (2000).

[3] J. H. Kim, H. Kim, D. Kim, Y. E. Ihm, and W. K. Choo, Physica B **327**, 304 (2003).

[4] Q. Xu, L. Hartmann, H. Schmidt, H. Hochmuth, M. Lorenz, R. Schmidt-Grund, D. Spemann, and M. Grundmann, J. Appl. Phys.(to be published).

[5] K.-W. Nielsen, J. B. Philipp, M. Opel, A. Erb, J. Simon, L. Alff, and R. Gross, Superlattices Microstruct. **37**, 327 (2005).
[6] T. Andrearczyk, J. Jaroszyński, G. Grabecki, T. Dietl, T. Fukumura, and M. Kawasaki, Phys. Rev. B **72**, 121309(R) (2005).
[7] T. Dietl, in *Semimagnetic Semiconductors and Diluted Magnetic Semiconductors*, edited by M. Averous and M. Balkanski (Plenum Press, New York, 1991), and references therein.
[8] J. Mycielski, in *Diluted Magnetic Semiconductors*, edited by J. K. Furdyna and J. Kossut, Semiconductors and Semimetals edited by R. K. Willardson and A. C. Beer, Vol. 25 (Academic Press, San Diego, 1988).
[9] R. Schmidt, B. Rheinländer, M. Schubert, D. Spemann, T. Butz, J. Lenzner, E. M. Kaidashev, M. Lorenz, A. Rahm, H. C. Semmelhack, and M. Grundmann, Appl. Phys. Lett. **82**, 2260 (2003).
[10] Y. G. Wang, S. P. Lau, H. W. Lee, S. F. Yu, B. K. Tay, X. H. Zhang, K. Y. Tse, and H. H. Hng, J. Appl. Phys. **94**, 1597 (2003).
[11] H. von Wenckstern, S. Weinhold, G. Biehne, R. Pickenhain, H. Schmidt, H. Hochmuth, and M. Grundmann, Adv. Solid State Phys. **45**, 263 (2005).
[12] J. S. Higgins, S. R. Shinde, S. B. Ogale, T. Venkatesan, and R. L. Greene, Phys. Rev. B **69**, 073201 (2004).
[13] P. A. Lee and T. V. Ramakrishnan, Rev. Mod. Phys. **57**, 287 (1985).
[14] C. Song, K. W. Geng, F. Zeng, X. B. Wang, Y. X. Shen, F. Pan, Y. N. Xie, T. Liu, H. T. Zhou, and Z. Fan, Phys. Rev. B **73**, 024405 (2006).